

## Conformation-space renormalization of randomly branched polymers

Shi-Min Cui

*Department of Physics, University of Waterloo, Waterloo, Ontario, Canada N2L 3G1*

Zheng Yu Chen

*Guelph-Waterloo Program for Graduate Work in Physics and Department of Physics, University of Waterloo, Waterloo, Ontario, Canada N2L 3G1*

(Received 10 April 1995)

We present a renormalization group theory in polymer conformation space to describe randomly branched polymers in which monomers interact with each other through the excluded volume interaction. We make a perturbation expansion for the mean square radius of gyration of randomly branched polymers with annealed structures and identify the appropriate scaling variable. We further perform a renormalization group analysis that results in the  $\epsilon$  expansion for the critical exponents of the radius of gyration  $\nu = \frac{1}{4} + \epsilon/36$  and of the number of configurations  $\theta = \frac{5}{2} - \epsilon/12$ , which are consistent with the results of an earlier theory.

PACS number(s): 61.25.Hq, 61.41.+e, 64.60.Ak

### I. INTRODUCTION

The theoretical description of the properties of polymer solutions with the excluded volume interaction is both fundamentally important and enormously challenging. For linear polymers, the renormalization group theory has been successful in understanding the essential universal characteristics of polymer solutions when the excluded volume interaction is present; there are a number of books that review various aspects of this subject [1–3]. In contrast, less is known about branched polymers [4–6], although deep connections are thought to exist between the problem and other areas of statistical mechanics, such as lattice animals [7] and Ising magnetic systems [8,9]. In view of a renewed interest in the subject [10–15], it is desirable to examine the configurational properties of branched polymers. In particular, randomly branched polymers with annealed branching points are studied in this paper by using an approach of conformational-space renormalization group (RG) theory.

Presently, three approaches that deal with the problem of calculating conformation properties of branched polymers are used in the literature. The first one is due to Zimm and Stockmayer [4], who formulated the problem by introducing the combinatorial mean-field analysis. The mean-field value for the critical exponent  $\nu$  of the mean-square radius of gyration was determined to be  $\frac{1}{4}$ . It is difficult, however, to generalize this approach to include the effect of the excluded volume interaction between monomers. The second approach is the one proposed by Lubensky and Isaacson [7], who studied a model that maps the lattice animal problem to a magnetic Hamiltonian functional in terms of an  $nm$ -component field variable where the limits  $n \rightarrow 0$  and  $m \rightarrow 0$  must be taken. They pointed out that the critical dimensionality for the problem is  $D_c = 8$  and used a RG technique to ob-

tain the  $\epsilon$  expansion for various critical exponents up to order  $\epsilon$ . Parisi and Sourlas [8] further applied this model to show that the critical exponents of animals in  $D$  dimensions are related to the exponents of the Lee-Yang edge singularity of the Ising model in an imaginary field in  $D - 2$  dimensions. They found an exact result for  $\nu$  in three dimensions when the excluded volume interaction is present,  $\nu(D=3) = \frac{1}{2}$ . However, this formalism lacks a direct mechanism for the calculation of the universal properties of the polymer problem, which do not have direct counterparts in the magnetic systems. The third formalism is due to an earlier suggestion by de Gennes [5], who directly examined the end-to-end distribution function in terms of graph representations of the integral. This method is quite useful because it has the advantage of explicitly maintaining the desired physical variables in the expressions. de Gennes found the mean-field value of  $\nu$ :  $\nu_{MF} = \frac{1}{4}$ , which is consistent with the value obtained by Zimm and Stockmayer [4]. In this paper, we present an approach of conformation-space RG theory based on de Gennes's original formalism, by considering the effect of the excluded volume interaction. Our main goals are (i) to find the appropriate scaling relations between various properties of interest and (ii) to formulate an approach for calculating the conformational properties of annealed branched polymers in the dilute limit.

The idea of constructing the conformation-space RG idea for linear polymers was first introduced by de Gennes [16]. Freed and co-workers [3,17] considered the polymer-chain conformation-space formalism for linear polymers with the theory represented in terms of the unperturbed Gaussian polymer distribution functions and the excluded volume interaction. This method has proven to be fruitful since it enables a systematic calculation of the physical quantities of linear polymers [3,17,18]. However, in the case of branched polymers, the unperturbed distribution function is non-Gaussian [5]. The

end-to-end distribution functions with specified internal points differ from the external end-to-end ones due to the branching. This problem is solved in this paper by taking possible branchings at the internal segments into consideration.

A number of issues are not addressed in this paper. First, we consider trifunctional branching units only, i.e., the branching points can have one (ends), two (linear parts), or three branches. We believe that our method can be extended for the consideration of  $f$ -functional branching units [4,7], which are not considered here. Second, we assume a model for randomly branched polymers without ring structures. Lubensky and Isaacson [7] noted that randomly branched polymers with ring structures belong to the same universality class as the ones without ring structures. Third, as in most of the previous works [4,5,7,15,19–21], we consider only the situation when the branching points are annealed, i.e., when the statistical distribution of the branching points is determined by maintaining the activity of the branching points constant. Recently, a Flory-like argument [11] and a Monte Carlo simulation [22] have demonstrated the possibility of the existence of another universality class for randomly branched polymers: those with quenched branching structures. As will be discussed elsewhere [23], our approach presented in this paper can be easily modified by using the replica method to describe quenched randomly branched polymers [12]. Finally, we are mainly interested in discussing the mean-square radius of gyration, the complete partition function, and the related critical exponents. Other physical quantities, such as elasticity, defined in Ref. [21], are not considered.

The plan of the paper is as follows. Section II describes the microscopic model. As the zeroth-order of our perturbation scheme, de Gennes' theory [5] for the end-to-end distribution function is also briefly reviewed. In Sec. III the correlation functions, with interior points specified, are explained and calculated; the results are then used to calculate the partition function, the mean-square radius of gyration, and the second virial coefficient to first order in excluded volume. The 't Hooft-Veltman dimensional regularization approach [24] is used for these calculations. In Sec. IV we present a general consideration of the conformation-space RG scheme and construct the RG equation for the mean-square radius of gyration. The exponents of the mean-square radius of gyration  $\nu$  and of the number of configurations  $\theta$  are evaluated to order  $\epsilon$ . Section V is devoted to the discussion. In Appendix A we discuss a comparison between the analytic mean-field results for the mean-square radius of gyration based on a direct calculation and the Kramers theorem [25]. Appendix B lists the correlation functions used in this paper. Appendix C shows the procedure for obtaining the critical dimensionality  $D_c = 8$  from the current model.

## II. BASIC FORMALISM

### A. Microscopic model

We consider a branched polymer of  $n$  branching points that divide the polymer into  $2n + 1$  linear portions, which

are separated by two tribranching points, or a tribranching point and an end (see Fig. 1). The polymer is assumed to have total contour length  $L$  and Kuhn length  $l$ , moving in a  $D$ -dimensional hyperspace of volume  $V$ . For each linear portion labeled by  $\kappa$  ( $\kappa = 1, 2, \dots, 2n + 1$ ), the statistical weight factor is chosen to obey the Gaussian distribution

$$g_\kappa[\mathbf{r}] = \frac{1}{(4\pi)^{D/2}} \exp \left[ -\frac{1}{4} \int_0^{L_\kappa} dt_\kappa \left| \frac{d\mathbf{r}(t_\kappa)}{dt_\kappa} \right|^2 \right]. \quad (2.1)$$

For convenience, here and hereinafter we utilize the variable  $\mathbf{r}(t_\kappa) \equiv (2D/l)^{1/2} \mathbf{R}(t_\kappa)$ , where  $\mathbf{R}(t_\kappa)$  designates the spatial position of the polymer segment at the contour position  $t_\kappa$  of the  $\kappa$ th portion with length  $L_\kappa$ . The complete canonical statistical distribution function can then be written as

$$P_s(n, L, [\mathbf{r}]) = \prod_{\kappa=1}^{2n+1} g_\kappa[\mathbf{r}] \exp(-v[\mathbf{r}]), \quad (2.2)$$

where  $v[\mathbf{r}]$  represents the excluded volume interaction potential

$$v[\mathbf{r}] = \frac{1}{2} u_0 \sum_{\kappa=1}^{2n+1} \sum_{\kappa'=1}^{2n+1} \int_0^{L_\kappa} dt_\kappa \int_0^{L_{\kappa'}} dt_{\kappa'} \delta[\mathbf{r}(t_\kappa) - \mathbf{r}(t_{\kappa'})]. \quad (2.3)$$

The constant  $u_0$  in Eq. (2.3) is the bare, i.e., unrenormalized, excluded volume parameter. The subscript  $s$  in Eq. (2.2) denotes the fact that the distribution function  $P_s(n, L, [\mathbf{r}])$  explicitly depends on the branching structure of the molecule.

For annealed randomly branched molecules, the number of tribranching points  $n$  is a fluctuating physical quantity. Instead, it is more natural to directly use the activity of the trifunctional unit  $\Lambda^2$  as a variable of the theory. Furthermore, because of the randomness of the branching structures, we may assume that all different

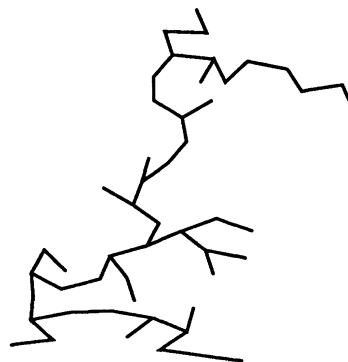


FIG. 1. Schematic diagram to illustrate a typical structure of a branched polymer. We consider trifunctional branching points only. In addition, the possibility of forming rings is ignored.

branching structures occur in the same frequency. Thus we consider the grand canonical distribution

$$P(\Lambda, L, [\mathbf{r}]) = \sum_{s, n} \Lambda^{2n} P_s(n, L, [\mathbf{r}]), \quad (2.4)$$

where the summation goes over all possible branching structures. The calculation presented in this article is based on the distribution function given in Eq. (2.4).

The introduction of the variable  $\mathbf{r}(t)$  is similar to the procedure introduced in studying linear polymers [3]. Taking the dimension of the contour length  $L$  as the fundamental dimension of the theory  $\lambda$ ,

$$[L] = \lambda, \quad (2.5)$$

one can determine the dimensions of all physical quantities involved in this paper. Since  $v[\mathbf{r}]$  in Eq. (2.2) is dimensionless, we may deduce

$$[\mathbf{r}] = \lambda^{1/2}, \quad (2.6)$$

$$[u_0] = \lambda^{D/2-2}, \quad (2.7)$$

$$[\Lambda] = \lambda^{-1}. \quad (2.8)$$

Note that the combinations  $[L/\Lambda] = \lambda^2$  and  $[u_0\Lambda^2] = \lambda^{-\epsilon/2}$ , where  $\epsilon = 8 - D$ .

The integral in Eq. (2.3) should be supplemented by the restriction that prohibits the contour distance of the two considered contour points from becoming smaller than a cutoff length  $a$ , which has the magnitude of the Kuhn length. Such a restriction eliminates possible singularities arising from self-excluded volume interactions of monomer units. As has been stressed by Freed [3] in the context of linear polymer chains,  $a$  is not necessarily the true microscopic minimum length and maybe thought of as an effective size of a real system.

### B. de Gennes' end-to-end distribution function

The theory, deduced when the excluded volume interaction is ignored, forms the basis for the perturbation scheme that will be established later. For completeness, we briefly review de Gennes' derivation for the end-to-end distribution function [5], which describes the probability of finding any two of the ends of the molecule being at the points with spatial coordinates  $\mathbf{r}$  and  $\mathbf{r}'$ ,

$$G_0(\mathbf{r}, \mathbf{r}'; L) = \int_{\mathbf{r}'}^{\mathbf{r}} \mathcal{D}[\mathbf{r}] P(\Lambda, L, [\mathbf{r}]). \quad (2.9)$$

Diagrammatically represented by the propagators in Fig. 2,  $G_0$  can be evaluated according to the basic definition in Eq. (2.4),

$$\begin{aligned} G_0(\mathbf{r}, \mathbf{r}'; L) &= g(\mathbf{r}, \mathbf{r}'; L) \\ &+ \Lambda^2 \int \int d\mathbf{r}_1 d\mathbf{r}_2 \sum_{L_1, L_2} g(\mathbf{r}, \mathbf{r}_1, L - L_1) \\ &\quad \times G_0(\mathbf{r}_1, \mathbf{r}', L_1 - L_2) \\ &\quad \times G_0(\mathbf{r}_1, \mathbf{r}_2; L_2), \end{aligned} \quad (2.10)$$

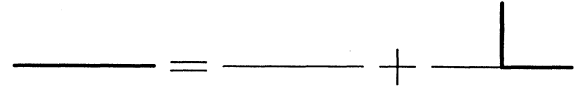


FIG. 2. Diagrammatic construction for the end-to-end distribution function, which is represented by the thick lines. The linear parts of the polymer with no branching point, which can be described by the Gaussian distribution, are represented by the thin lines.

where  $g$  denotes a Gaussian distribution corresponding to the linear part of the polymer [1]. The introduction of the Fourier and Laplace transformations

$$\begin{aligned} \tilde{G}_0(\mathbf{k}; p) &= \int \frac{d^D \mathbf{k}}{(2\pi)^D} \exp[i\mathbf{k} \cdot (\mathbf{r} - \mathbf{r}')] \\ &\quad \times \int_0^\infty dL \exp(-pL) G_0(\mathbf{r}, \mathbf{r}'; L) \end{aligned} \quad (2.11)$$

leads to

$$\tilde{G}_0(\mathbf{k}; p) = \bar{g}(\mathbf{k}; p) + \Lambda^2 \bar{g}(\mathbf{k}; p) \tilde{G}_0(\mathbf{k}; p) \tilde{G}_0(0; p), \quad (2.12)$$

where

$$\bar{g}(\mathbf{k}; p) = \frac{1}{\mathbf{k}^2 + p} \quad (2.13)$$

is the Gaussian distribution in the Fourier and Laplace representations. The solution of Eq. (2.12) is [5]

$$\tilde{G}_0(\mathbf{k}; p) = \frac{1}{\mathbf{k}^2 + [p + (p^2 - 4\Lambda^2)^{1/2}]/2}. \quad (2.14)$$

Based on this solution, the grand partition function  $G_0(L)$  can be evaluated

$$G_0(L) = \mathcal{L}_L^{-1} \tilde{G}_0(0, p) = \frac{I_1(2\Lambda L)}{\Lambda L}, \quad (2.15)$$

where  $\mathcal{L}_L^{-1}$  denotes the inverse Laplace transformation and  $I_m(x)$  the  $m$ th-order modified Bessel function of the first kind. The averaged number of branched points  $\bar{n}$  can then be deduced

$$\bar{n} = \Lambda^2 \frac{\partial}{\partial \Lambda^2} \ln G_0(L) \approx \Lambda L, \quad \Lambda L \gg 1. \quad (2.16)$$

Following the Kramers theorem [25] and its generalization, de Gennes [5] calculated the mean-square radius of gyration  $\bar{S}^2$  and Daoud and Joanny [21] calculated  $\bar{S}^4$ . However, the mean-square radius of gyration can also be calculated based on the very definition of the scattering structure factor. We give a more detailed discussion of the derivation in Appendix A. Making use of the large- $z$  expansion of the modified Bessel function  $I_m(z)$ , we obtain the large- $\Lambda L$  behavior of  $\bar{S}^2$

$$\bar{S}^2 = \frac{LD}{2} \left[ \frac{\pi L}{\Lambda} \right]^{1/4}. \quad (2.17)$$

The mean-field critical exponent is then

$$\nu_{\text{MF}} = \frac{1}{4}. \quad (2.18)$$

III. PERTURBATION CALCULATION

A. Correlation function and perturbation expansion

Due to the possibility of branching, the excluded volume problem of randomly branched polymers is more complicated than that of linear polymers. For linear polymers, the perturbation expansion in  $u_0$  can be formulated by implementing the standard Feynman diagram technique since the two-point correlation function is simply Gaussian. For branched polymers, de Gennes' unperturbed end-to-end distribution function is non-Gaussian and possible branching at an interior segment must be

taken into account.

In order to carry out the perturbation expansion in  $u_0$  of the physical properties of interest, we must introduce the correlation functions  $G_l(\mathbf{r}, \mathbf{r}'; \mathbf{r}_1, \mathbf{r}_2, \dots, \mathbf{r}_l; L)$ ,  $l=0, 1, 2, \dots$ , for randomly branched polymers when the  $l$  internal points have the positions denoted by the vectors  $\mathbf{r}_1, \mathbf{r}_2, \dots, \mathbf{r}_l$  and the two external ends have the positions denoted by the vectors  $\mathbf{r}$  and  $\mathbf{r}'$ . The function  $G_l$  can be evaluated based on the basic definition of the probability function in Eq. (2.4).

To illustrate how  $G_l$  is calculated, we give here the example of calculating  $G_1(\mathbf{r}, \mathbf{r}'; \mathbf{r}_1; L)$ . According to the distribution function,  $G_1$  can be written as

$$G_1(\mathbf{r}, \mathbf{r}'; \mathbf{r}_1; L) = \sum_{L_1} g(\mathbf{r}, \mathbf{r}_1; L_1) g(\mathbf{r}_1, \mathbf{r}'; L - L_1) + \Lambda^2 \int \int d\mathbf{r}'_1 d\mathbf{r}'_2 \sum_{L_1, L_2} \left[ \sum_{L_3} g(\mathbf{r}, \mathbf{r}_1; L_3) g(\mathbf{r}_1, \mathbf{r}'_1; L - L_1 - L_3) G_0(\mathbf{r}'_1, \mathbf{r}'; L_1 - L_2) g(\mathbf{r}'_1, \mathbf{r}'_2; L_2) + g(\mathbf{r}, \mathbf{r}'_1; L - L_1) G_1(\mathbf{r}'_1, \mathbf{r}'; \mathbf{r}_1; L_1 - L_2) G_0(\mathbf{r}'_1, \mathbf{r}'_2; L_2) + g(\mathbf{r}, \mathbf{r}'_1; L - L_1) G_0(\mathbf{r}'_1, \mathbf{r}'; L_1 - L_2) G_1(\mathbf{r}'_1, \mathbf{r}'_2; \mathbf{r}_1; L_2) \right]. \tag{3.1}$$

A convenient way of understanding the various terms in Eq. (3.1) is to associate each term with a corresponding graph [Fig. 3(a)]. The thick line in Fig. 3(a) with the interior point specified by a diamond represents  $G_1$ . It is obvious that the first three graphs can be combined to simplify the graph by making use of Fig. 2 inasmuch as the corresponding terms in Eq. (3.1) can be combined into a simple form according to Eq. (2.10). We then have a more compact form of  $G_1$

$$G_1(\mathbf{r}, \mathbf{r}'; \mathbf{r}_1; L) = \sum_{L_1} G_0(\mathbf{r}, \mathbf{r}_1; L - L_1) G_0(\mathbf{r}_1, \mathbf{r}'; L_1) + \Lambda^2 \sum_{L_1, L_2} \int \int d\mathbf{r}'_1 d\mathbf{r}'_2 G_0(\mathbf{r}, \mathbf{r}'_1; L - L_1) \times G_0(\mathbf{r}'_1, \mathbf{r}'; L_1 - L_2) \times G_1(\mathbf{r}'_1, \mathbf{r}'_2; \mathbf{r}_1; L_2), \tag{3.2}$$

which can be represented diagrammatically by Fig. 3(b). In view of the graph representation, we may say that the second term in the expression (3.2) for  $G_1$  comes from the branching that may occur at  $\mathbf{r}_1$ . The Fourier and Laplace transformation of Eq. (3.2) becomes

$$\tilde{G}_1(\mathbf{k}_1, \mathbf{k}_2; \mathbf{k}_3; p) = [\tilde{G}_0(\mathbf{k}_1; p) \tilde{G}_0(\mathbf{k}_2; p) + \Lambda^2 \tilde{G}_0(\mathbf{k}_1; p) \tilde{G}_0(\mathbf{k}_2; p) \times \tilde{G}_1(0, \mathbf{k}_3; \mathbf{k}_3; p)] (2\pi)^D \times \delta(\mathbf{k}_1 + \mathbf{k}_2 + \mathbf{k}_3). \tag{3.3}$$

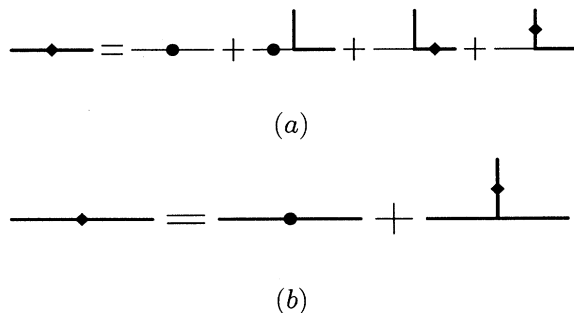


FIG. 3. Diagrammatic representation for  $G_1(\mathbf{r}, \mathbf{r}'; \mathbf{r}_1; L)$  in (a) Eq. (3.1) and (b) Eq. (3.2). The filled diamond denotes possible branching at an interior point and the filled circle denotes a nonbranched interior point. The two sets of graphs are equivalent.

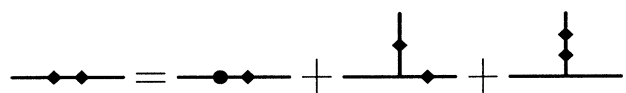


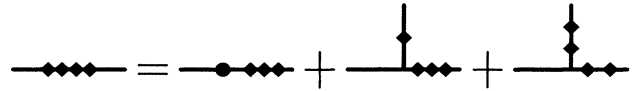
FIG. 4. Diagrammatic representation for  $G_2(\mathbf{r}, \mathbf{r}'; \mathbf{r}_1, \mathbf{r}_2; L)$ .

FIG. 5. Diagrammatic representation for  $G_3(\mathbf{r}, \mathbf{r}'; \mathbf{r}_1, \mathbf{r}_2, \mathbf{r}_3; L)$ .

The solution of Eq. (3.3) for the function  $\tilde{G}_1$  is found to be

$$\tilde{G}_1(\mathbf{k}_1, \mathbf{k}_2; \mathbf{k}_3; p) = \frac{\tilde{G}_0(\mathbf{k}_1; p) \tilde{G}_0(\mathbf{k}_2; p) (2\pi)^D \delta(\mathbf{k}_1 + \mathbf{k}_2 + \mathbf{k}_3)}{1 - \Lambda^2 \tilde{G}_0(\mathbf{k}_3; p) \tilde{G}_0(0; p)}. \quad (3.4)$$

We now proceed to the evaluation of the expressions for the correlation functions  $G_l$  ( $l=2,3,4$ ) that are needed to carry out the perturbation calculation of various physical properties of interest. The derivation can be done in the same way. The results for  $G_2$ ,  $G_3$ , and  $G_4$  are represented graphically by Figs. 4, 5, and 6, respectively. We observe that the graphs associated with  $G_l(\mathbf{r}, \mathbf{r}'; \mathbf{r}_1, \mathbf{r}_2, \dots, \mathbf{r}_l; L)$  can be categorized into three groups: (i) for a given  $l$ , a graph that represents  $G_0 G_{l-1}$  can be deduced (see the first graphs in Figs. 4–6); (ii) different ways of arranging  $G_{l_1}$  and  $G_{l_2}$  for the two arms of the branched graphs ( $l_1 + l_2 = l$ ,  $l_1 \geq 1$ ,  $l_2 \geq 1$ ) must be considered; and finally (iii) a graph represents the possible choice of  $(\mathbf{r}_1, \mathbf{r}_2, \dots, \mathbf{r}_l)$  indirectly related to the path

FIG. 6. Diagrammatic representation for  $G_4(\mathbf{r}, \mathbf{r}'; \mathbf{r}_1, \mathbf{r}_2, \mathbf{r}_3, \mathbf{r}_4; L)$ .

connecting  $\mathbf{r}$  and  $\mathbf{r}'$  may be considered (see the last graphs in Figs. 4–6). Appendix B contains the algebraic expressions for  $G_2$ ,  $G_3$ , and  $G_4$ . It is worthwhile to note that these expressions reduce to the corresponding correlation functions of a linear Gaussian chain in the limiting case of  $\Lambda=0$  [3].

To conclude this section, we give the example of evaluating the partition function, which can be expressed as an asymptotic expansion in powers of the excluded volume parameter  $u_0$ . We obtain

$$G_B(L) = G_B^{(0)}(L) + \sum_{m=1}^{\infty} G_B^{(m)}(L), \quad (3.5)$$

with

$$G_B^{(m)}(L) = \frac{(-u_0)^m}{2!(2m-2)!} \int d^D \mathbf{r} \int d^D \mathbf{r}' \int d^D \mathbf{r}_1 \cdots \int d^D \mathbf{r}_{2m} G_{2m}(\mathbf{r}, \mathbf{r}'; \mathbf{r}_1, \mathbf{r}_2, \dots, \mathbf{r}_{2m}; L) \times \delta(\mathbf{r}_1 - \mathbf{r}_2) \cdots \delta(\mathbf{r}_{2m-1} - \mathbf{r}_{2m}), \quad (3.6)$$

where the subscript  $B$  denotes bare function. In the Fourier-Laplace space, Eq. (3.5) becomes

$$\tilde{G}_B(p) = \tilde{G}_B^{(0)}(p) + \sum_{m=1}^{\infty} \tilde{G}_B^{(m)}(p), \quad (3.7)$$

with

$$\tilde{G}_B^{(m)}(p) = \frac{(-u_0)^m}{2!(2m-2)!} \int \frac{d^D \mathbf{k}_1}{(2\pi)^D} \cdots \int \frac{d^D \mathbf{k}_m}{(2\pi)^D} \tilde{G}_{2m}(0, 0; \mathbf{k}_1, -\mathbf{k}_1, \dots, \mathbf{k}_m, -\mathbf{k}_m; p). \quad (3.8)$$

The correlation function in the integrand can be found in Appendix B.

### B. Dimensional regularization

As mentioned earlier, the microscopic model in Sec. II A should be restricted to describing randomly branched polymers interacting at a distance greater than the microscopic length  $a$ . Because of the particular functional form of the Gaussian distribution of the linear part

of the polymer, the present model may produce diverging singularities in the limit of  $a \rightarrow 0$  when various physical quantities are calculated. These divergences depend on the value of  $a$  and also on the regularization scheme, i.e., the form that is used to impose the cutoff (hard cutoff, smooth cutoff, etc.).

In general, the integral appearing in the model contains singularities when  $D=4, 6, 8, \dots$  is approached. The divergences at  $D=4$  and  $6$ , however, can be absorbed by redefining the basic parameters perturbatively

in the model, as demonstrated in Appendix C. The parameters highly depend on the microscopic details of the model. The divergences at the critical dimension  $D_c = 8$ , however, must be dealt with by introducing a RG transformation. It is this dimensionality that interests us the most: the universal scaling behavior and critical exponent are closely associated with  $D_c = 8$

The dimensional regularization scheme, suggested by 't Hooft and Veltman [24] and subsequently applied to the RG analyses of many models for critical systems, is a powerful technique to extract the singularities near  $D_c = 8$ . The other microscopic details relating to the divergences at  $D = 4$  and 6 are simply suppressed. To use the dimensional regularization, one first formally calculates the integral at low dimensions and then expands the resulting expression near the critical dimension. We adopt the dimensional regularization scheme in this work.

**C. Partition function**

The first-order contribution in  $u_0$  to  $G_B$  is related to  $G_2$

$$\tilde{G}_B^{(1)}(p) = -\frac{u_0}{2!0!} \int \frac{d^D \mathbf{k}}{(2\pi)^D} \tilde{G}_2(0, 0; \mathbf{k}, -\mathbf{k}; p). \quad (3.9)$$

Diagrammatically, it can be represented by the one-loop graph in Fig. 7, where the dashed curve describes the contraction due to the  $\delta$ -function-type interaction. For  $D \geq 4$  the integral in Eq. (3.9) is formally divergent due to the neglect of an ultraviolet cutoff in Eq. (2.3). To extract the singular portion, we use the dimensional regularization scheme

$$\int \frac{d^D \mathbf{k}}{(2\pi)^D} \frac{1}{(k^2 + t)^m} = \frac{\Gamma(m - D/2)}{(4\pi)^{D/2} \Gamma(m)} t^{D/2 - m}. \quad (3.10)$$

We then have

$$\tilde{G}_B^{(1)}(p) = -\frac{u_0 \Gamma(2 - D/2)}{(4\pi)^{D/2} \Gamma(2)} (p^2 - 4\Lambda^2)^{D/2 - 3} + \dots, \quad (3.11)$$

where  $\Gamma(m)$  is the Gamma function. Here we retain only the term that contributes most significantly in  $L$  when Eq. (3.11) is transformed back to the  $L$  space. A direct inverse Laplace transform of Eq. (3.11) yields the partition function at large  $L$



FIG. 7. Expansion for the partition function in  $u_0$  up to one loop. The dashed line represents the excluded volume interaction, which can be characterized by the interaction parameter  $u_0$ , between the two points specified by the diamonds.

$$\frac{G_B(L)}{G_B^{(0)}(L)} = 1 - \frac{u_0 \Lambda^2 \Gamma(1 - D/4)}{2(4\pi)^4} \left[ \frac{16\pi^2 L}{\Lambda} \right]^{\epsilon/4}. \quad (3.12)$$

Note that the combination of the parameters

$$z = \frac{u_0 \Lambda^2}{(4\pi)^4} \left[ \frac{16\pi^2 L}{\Lambda} \right]^{\epsilon/4} \quad (3.13)$$

appears in Eq. (3.12). Expanding Eq. (3.12) to order  $\epsilon^0$  yields

$$\frac{G_B(L)}{G_B^{(0)}(L)} = 1 + \frac{2u}{\epsilon} \left[ 1 + \frac{\epsilon}{4} \left[ 1 - \gamma + \ln \frac{16\pi^2 L}{\lambda^2 \Lambda} \right] \right], \quad (3.14)$$

where  $\gamma$  is the Euler's constant and  $u$  is the dimensionless coupling constant defined by

$$u = \frac{u_0 \Lambda^2 \lambda^{\epsilon/2}}{(4\pi)^4}. \quad (3.15)$$

**D. Second virial coefficient**

To calculate the second virial coefficient, it is necessary to consider the interaction between two branched polymers. The bare second virial coefficient  $A_{2B}$  is given by

$$A_{2B} = \frac{\int d^D \mathbf{r}_1 \int d^D \mathbf{r}_2 \int d^D \mathbf{r}'_1 \int d^D \mathbf{r}'_2 \mathcal{G}_c(\mathbf{r}_1, \mathbf{r}_2, \mathbf{r}'_1, \mathbf{r}'_2)}{G_B^2}, \quad (3.16)$$

where  $\mathcal{G}_c$  is the connected, two-chain correlation function, when polymer 1 has its ends at  $\mathbf{r}_1$  and  $\mathbf{r}'_1$  and polymer 2 at  $\mathbf{r}_2$  and  $\mathbf{r}'_2$ .

Now, expanding Eq. (3.16) in powers of  $u_0$ , we are able to express  $A_{2B}$  in terms of the correlation functions defined in Sec. III A. We may use the diagrammatic representation for the involved integral as in Fig. 8, which is self-explanatory. The first-order diagram shown in Fig. 8 is associated with the correlation function  $G_1$ , which in the Fourier-Laplace space is given by

$$\mathcal{G}_c^{(1)} = u_0 \tilde{G}_1(0, 0; 0; p) \tilde{G}_1(0, 0; 0; p'). \quad (3.17)$$

Performing the inverse Laplace transformation yields the first-order contribution at large  $L$  in the  $L$  space

$$\mathcal{G}_c^{(1)} = u_0 L^2 [G_B^{(0)}(L)]^2. \quad (3.18)$$

The second diagram appearing in Fig. 8 involves the calculation of the integral containing  $G_2$ . Analytically, we

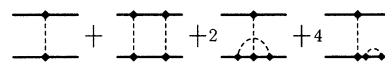


FIG. 8. Expansion for the connected, two-chain correlation function in  $u_0$  up to one loop, which is used to evaluate the second virial coefficient.

have

$$\begin{aligned} \tilde{G}_c^{(2a)} = & -\frac{2u_0^2}{(2!0!)^2} \int \frac{d^D \mathbf{k}}{(2\pi)^D} \tilde{G}_2(0,0;\mathbf{k},-\mathbf{k};p) \\ & \times \tilde{G}_2(0,0;\mathbf{k},-\mathbf{k};p'). \end{aligned} \quad (3.19)$$

Carrying out the integral and performing the inverse Laplace transformation yields

$$\begin{aligned} G_c^{(2a)} = & -\frac{2u_0^2 L^2 \Lambda^2}{3(4\pi)^4 \epsilon} [G_B^{(0)}(L)]^2 \\ & \times \left[ \frac{16\pi^2 L}{\Lambda} \right]^{\epsilon/4} [1 + O(\epsilon)]. \end{aligned} \quad (3.20)$$

Note that terms of order  $[G_B^{(0)}(L)]L^{1+\epsilon/4}$  or lower are negligible at large  $L$ . The last two diagrams appearing in Fig. 8 are associated with  $G_1$  and  $G_3$ . The computation of the integral represented by these two graphs proceeds in the same manner. This leads to

$$G_c^{(2b)} = \frac{4u_0^2 L^2 \Lambda^2}{(4\pi)^4 \epsilon} [G_B^{(0)}(L)]^2 \left[ \frac{16\pi^2 L}{\Lambda} \right]^{\epsilon/4} [1 + O(\epsilon)]. \quad (3.21)$$

Now, grouping the different graphs in Fig. 8, we obtain the second virial coefficient up to order  $u_0^2$

$$A_{2B} = u_0 L^2 \left[ 1 - \frac{2u}{3\epsilon} \left[ \frac{16\pi^2 L}{\lambda^2 \Lambda} \right]^{\epsilon/4} [1 + O(\epsilon)] \right] + O(u_0^3). \quad (3.22)$$

### E. Mean square radius of gyration

The bare mean-square radius of gyration can be evaluated through  $\mathcal{S}(\mathbf{k}, L)$ , the coherent-scattering structure factor,

$$\overline{S_B^2} = -\frac{l}{2} \frac{\sum_{i=1}^D \partial^2 \mathcal{S}_B(\mathbf{k}, L) / \partial k_i^2}{\mathcal{S}_B(\mathbf{k}, L)} \Big|_{\mathbf{k}=0}, \quad (3.23)$$

where  $\mathcal{S}(\mathbf{k}, L)$  is defined as

$$\begin{aligned} \mathcal{S}_B(\mathbf{k}, L) & = \left\langle \frac{1}{2} \sum_{\kappa, \kappa'} \int_0^{L_\kappa} dt_\kappa \int_0^{L_{\kappa'}} dt_{\kappa'} \exp\{i\mathbf{k} \cdot [\mathbf{r}(t_\kappa) - \mathbf{r}(t_{\kappa'})]\} \right\rangle, \end{aligned} \quad (3.24)$$

with  $\langle \rangle$  denoting the average with respect to the distribution given by Eq. (2.4). We can now expand  $\mathcal{S}_B$  in terms of powers of  $u_0$ . The resulting expression may be easily understood by using Fig. 9.

The zeroth-order term of  $\mathcal{S}_B(\mathbf{k}, L)$  is directly related to  $G_2$  in the  $\mathbf{k}$  space (see Fig. 9)

$$\tilde{\mathcal{S}}_B^{(0)}(\mathbf{k}, p) = \frac{1}{2!0!} \tilde{G}_2(0,0;\mathbf{k},-\mathbf{k};p). \quad (3.25)$$



FIG. 9. Expansion for the scattering structure factor in  $u_0$  up to one loop, which is used to calculate the mean square radius of gyration.

Taking derivatives according to Eq. (3.23), we obtain  $\overline{S_B^{(0)}} = lD(\pi L/\Lambda)^{1/4}/2$ .

The first-order contribution is related to  $G_4$ , whose expression appears in Appendix B,

$$\tilde{\mathcal{S}}_B^{(1)}(\mathbf{k}, p) = -\frac{u_0}{(2!)^2} \int \frac{d^D \mathbf{k}'}{(2\pi)^D} \tilde{G}_4(0,0;\mathbf{k},-\mathbf{k},\mathbf{k}',-\mathbf{k}';p). \quad (3.26)$$

The calculation of  $\tilde{\mathcal{S}}_B^{(1)}$  is more involved, but in the same manner as the calculation for other one-loop integral. We obtain, for large  $L$ , the expression for  $\overline{S_B^{(1)}}$ , which leads to

$$\begin{aligned} \overline{S_B^2} = & \frac{lD}{2} \left[ \frac{\pi L}{\Lambda} \right]^{1/2} \left[ 1 + \frac{4u}{3\epsilon} \left[ \frac{16\pi^2 L}{\lambda^2 \Lambda} \right]^{\epsilon/4} (1 - 0.108\epsilon) \right] \\ & + O(u_0^2). \end{aligned} \quad (3.27)$$

### F. Summary

In this section, we obtained the first-order corrections to the mean-field behavior of the partition function  $G(L)$ , the second virial coefficient  $A_2$ , and the mean-square radius of gyration  $\overline{S^2}$ , in the asymptotic expansion in powers of  $u_0$ , under the dimensional regularization scheme. The resulting expressions, Eqs. (3.17), (3.22), and (3.27), show that the appropriate, naturally produced scaling parameter is

$$z = \frac{u_0 \Lambda^2}{(4\pi)^4} \left[ \frac{16\pi^2 L}{\Lambda} \right]^{\epsilon/4}. \quad (3.28)$$

Although this scaling parameter is found through the procedure of dimensional regularization, we believe a similar definition can be made when the model is treated with an explicit cutoff for small  $a$ . A similar situation is found for the problem of linear polymers, where the basic scaling parameter appears to have the same form in both the expression deduced from the dimensional regularization scheme [3] and the perturbation expression when  $a \sim l$  is explicitly introduced [26]. This consideration prompted us to rescale the Monte Carlo simulation data [22] of  $\overline{S^2}$  obtained through an off-lattice algorithm, in which the parameter  $u_0$  can vary, according to the  $z$  parameter defined in Eq. (3.28). We have found that the Monte Carlo data indeed scale as expected for large  $\Lambda L$ .

## IV. RENORMALIZATION GROUP CALCULATION

### A. Renormalization

According to the basic assumption of the RG approach to critical phenomena, the microscopic details,

characterized by the value of the microscopic length  $a$ , are irrelevant to the universal behavior that occurs at macroscopic scale. The existence of the invariance in performing the RG transformation is the essential mechanism that produces the universal behavior.

The microscopic parameters contained in our model are the contour length  $L$ , the excluded volume  $u_0$ , and the tribranching activity  $\Lambda^2$ . The explicit calculations of the mean-square radius and the second virial coefficient, given in Sec. III, have shown that at large  $L$  they are all functions of the following two parameters  $M$  and  $u$  defined by

$$M = \frac{L}{\Lambda} \tag{4.1}$$

and

$$u = \frac{u_0 \Lambda^2 \lambda^{\epsilon/2}}{(4\pi)^4} . \tag{4.2}$$

Though we only performed the calculation up to one-loop order, we assume that  $M$  and  $u$  are the two fundamental microscopic parameters in our model.

Consider a certain bare quantity  $F_B(M, u, a)$  as a function of  $M, u$ , and the microscopic length  $a$ . The singularities that show up in  $F_B$  may be removed by defining the corresponding normalized quantities, so that the renormalized

$$F_r = F_r(M_r, u_r) \tag{4.3}$$

is independent of  $a$ . The normalized variables are related to the unnormalized ones in a linear form

$$M_r = Z_M M , \tag{4.4}$$

$$u_r = Z_u^{-1} u , \tag{4.5}$$

$$F_r = Z^{-1} F , \tag{4.6}$$

where the normalization coefficients  $Z_M, Z_u$ , and  $Z$  are assumed to be functions of  $u_r$ .

In Sec. III we consider a perturbation method to evaluate physical quantities by using the dimensional regularization scheme [24]. In general, the quantity  $F_B$  may be expressed by a series in powers of the dimensionless quantities  $uM^{\epsilon/4}$  and  $\epsilon$ ,

$$F_B = \sum_{m=0}^{\infty} \sum_n^{\infty} F_{mn}^B (uM^{\epsilon/4})^m \epsilon^n . \tag{4.7}$$

Note that the second summation in Eq. (4.7) may contain negative powers of  $n$ . In writing down Eq. (4.7), we made the assumption that high-order loop graphs contribute to  $F_B$  in the similar way as the one-loop result.

Writing  $Z_M, Z_u$ , and  $Z$  in the Taylor-expansion forms

$$Z_M = 1 + \sum_{m=1}^{\infty} a_m u_r^m , \tag{4.8}$$

$$Z_u = 1 + \sum_{m=1}^{\infty} b_m u_r^m , \tag{4.9}$$

$$Z = 1 + \sum_{m=1}^{\infty} d_m u_r^m , \tag{4.10}$$

we can now use the perturbation series of  $G(L), \overline{S^2}$ , and  $A_2$  to determine the coefficients  $a_m, b_m, \dots$ , to each order in  $u_r$ . Since there are many ways of keeping the renormalized functions finite, there are different ways of choosing the constant  $Z_M, Z_u$ , and  $Z$ . Here, in order to eliminate the singularities in  $\epsilon$ , a minimal subtraction of dimensional poles is assumed. The resulting  $F$  is well defined at  $\epsilon=0$  in the series

$$F = \sum_{m=0}^{\infty} \sum_{n=0}^{\infty} F_{mn} (u_r M_r^{\epsilon/4})^m \epsilon^n . \tag{4.11}$$

Since  $u_r$  turns out to be of order  $\epsilon$  in the macroscopic limit, to determine quantities  $F$  to order  $\epsilon$ , we only need to calculate the first-order coefficients  $a_1, b_1, \dots$ .

All the necessary terms for renormalizing are now available to first order in  $u$ . The singularities  $1/\epsilon$  in the bare quantities [see Eqs. (3.17), (3.22), and (3.27)] are required to be absorbed through Eqs. (4.3), (4.5), and (4.6). To the first order in  $u$ , we obtain  $a_1 = 8/3\epsilon, b_1 = 6/\epsilon$ , and  $d_1 = 2/\epsilon$  and thus

$$Z_M = 1 + \frac{8u_r}{3\epsilon} + O(u_r^2) , \tag{4.12}$$

$$Z_u = 1 + \frac{6u_r}{\epsilon} + O(u_r^2) , \tag{4.13}$$

and

$$Z = 1 + \frac{2u_r}{\epsilon} + O(u_r^2) . \tag{4.14}$$

### B. RG equation

As an example, we consider the mean-square radius of gyration  $\overline{S^2}$ , which is found to be a function of  $M, u$ , and  $\epsilon$ :

$$\overline{S_B^2} = \overline{S_B^2}(M, u, \epsilon) . \tag{4.15}$$

The corresponding macroscopic gyration  $\overline{S^2}$  should be equal to  $\overline{S_B^2}$ ,

$$\overline{S^2}(M_r, u_r, \lambda, \epsilon) = \overline{S_B^2}(M, u, \epsilon) \tag{4.16}$$

or simply

$$\overline{S^2}(M_r, u_r, \lambda, \epsilon) = \overline{S_B^2}(Z_M^{-1} M_r, Z_u u_r, \epsilon) . \tag{4.17}$$

On the other hand, using the system of units given by Eqs. (2.5)–(2.8), pure dimensional analysis yields

$$\overline{S^2} = s \overline{S^2} \left[ \frac{M_r}{s^2}, u_r, \frac{\lambda}{s}, \epsilon \right] \tag{4.18}$$

for any scaling constant  $s > 0$ .

The existence of a renormalized theory and the independence of  $\overline{S_B^2}$  on the macroscopic scale  $\lambda$  imply

$$\lambda \frac{\partial}{\partial \lambda} \overline{S_B^2}(M, u, \epsilon) = 0 . \tag{4.19}$$

Noting that  $Z_M$  and  $Z_u$  depend on  $\lambda$ , we have the RG equation



$$\left[ \lambda \frac{\partial}{\partial \lambda} + \beta(u_r) \frac{\partial}{\partial u_r} + \gamma(u_r) M_r \frac{\partial}{\partial M_r} \right] \bar{S}^2(M_r, u_r, \lambda, \epsilon) = 0, \quad (4.20)$$

where  $\beta(u_r)$  and  $\gamma(u_r)$  are the normalization functions

$$\beta(u_r) = \lambda \frac{\partial}{\partial \lambda} u_r, \quad (4.21)$$

$$\gamma(u_r) = \lambda \frac{\partial}{\partial \lambda} \ln Z_M. \quad (4.22)$$

The solution of the RG equation has been extensively studied before [24]. It gives rise to the asymptotic power law and thus may be used to determine the critical exponents. The change of the function  $\bar{S}^2$  under a change of  $\lambda$  becomes rather simple in a special case, namely, when

$$\beta^* = \beta(u_r^*) = 0, \quad (4.23)$$

where  $u_r^*$  is the fixed point coupling constant. At the fixed point  $u_r = u_r^*$ , Eq. (4.20) becomes

$$\left[ \lambda \frac{\partial}{\partial \lambda} + \gamma^* M_r \frac{\partial}{\partial M_r} \right] \bar{S}^2(M_r, u_r^*, \lambda, \epsilon) = 0, \quad (4.24)$$

with the numerical constant  $\gamma^*$

$$\gamma^* = \gamma(u_r^*). \quad (4.25)$$

The general solution of Eq. (4.24) at the fixed point is

$$\bar{S}^2 = \bar{S}^2 \left[ \frac{M_r}{\lambda^{\gamma^*}}, u_r^*, \epsilon \right]. \quad (4.26)$$

Comparing Eqs. (4.26) and (4.18) gives

$$\bar{S}^2 = s \bar{S}^2 \left[ \frac{M_r}{s^2} \left[ \frac{s}{\lambda} \right]^{\gamma^*}, u_r^*, \epsilon \right]. \quad (4.27)$$

Choosing  $s$  to be given by

$$\frac{M_r}{s^2} \left[ \frac{s}{\lambda} \right]^{\gamma^*} = 1, \quad (4.28)$$

we obtain the scaling law for  $\bar{S}^2$ ,

$$\bar{S}^2 = M_r^{1/(2-\gamma^*)} \lambda^{-\gamma^*/(2-\gamma^*)} f(u_r^*, \epsilon), \quad (4.29)$$

where  $f$  is an unknown function to be determined. The gyration exponent  $\nu$  defined by  $\bar{S}^2 \sim L^{2\nu}$  at large  $L$  is thus given according to Eq. (4.29) by

$$\nu = \frac{1}{4-2\gamma^*}. \quad (4.30)$$

The above derivation of the scaling law does not require the introduction of the perturbation expansion (3.5), so that the scaling law follows quite generally from the assumption of the existence of renormalized quantities and microscopic scale invariance.

Substituting Eqs. (4.12) and (4.13) into the definition of  $\beta$  and  $\gamma$  in Eqs. (4.21) and (4.22) yields

$$\beta(u_r) = \frac{\epsilon}{2} u_r - 3u_r^2 + O(u_r^3) \quad (4.31)$$

and

$$\gamma(u_r) = \frac{4}{3} u_r + O(u_r^2). \quad (4.32)$$

The fixed point  $u^*$  is determined from the definition  $\beta^* = 0$ ,

$$u_r^* = \frac{\epsilon}{6} + O(\epsilon^2). \quad (4.33)$$

Introducing (4.33) into (4.32) enables us to obtain

$$\gamma^* = \frac{2}{3} \epsilon + O(\epsilon^2). \quad (4.34)$$

The gyration exponent can be obtained from Eqs. (4.30) and (4.34) as

$$\nu = \frac{1}{4} \left[ 1 + \frac{\epsilon}{9} + O(\epsilon^2) \right]. \quad (4.35)$$

After renormalization, the expression for  $\bar{S}^2$  at large  $M_r$  can be written as

$$\bar{S}^2 = \frac{ID}{2} (\pi M_r)^{1/2} \left[ \frac{16\pi^2 M_r}{\lambda^2} \right]^{\epsilon/18} (1 - 0.007\epsilon). \quad (4.36)$$

The critical exponent that characterizes the number of configurations is related to the partition function  $G(L)$  by

$$G(L) \sim L^{1-\theta} b^L, \quad (4.37)$$

where  $b$  is a constant. From Eqs. (4.13) and (4.14), we can also deduce  $\theta$  by going through an analysis similar to that of  $\bar{S}^2$ . We have

$$\theta = \frac{5}{2} - \frac{\epsilon}{12}. \quad (4.38)$$

## V. DISCUSSION

We have developed a direct conformation-space approach by employing the RG technique to study randomly branched polymers. The method developed here echoes a similar idea in the study of the conformational properties of linear polymers [3]. The basic ingredients of the formalism are de Gennes' unperturbed distribution function for branched polymers [5], which assumes a Gaussian distribution for the linear part of the polymer and a  $\delta$ -function-type interaction between segments in the branched polymer, which is characterized by the exclude volume  $u_0$ . Such an approach has the advantages of explicitly maintaining the desired physical variables in various expressions and producing the proper scaling relations between various properties. The most important result is that the mean-square radius of gyration has a scaling form as

$$\bar{S}^2 \sim \left[ \frac{L}{\Lambda} \right]^{1/2} z^{2(4\nu-1)/\epsilon}, \quad (5.1)$$

where

$$z = \frac{u_0 \Lambda^2}{(4\pi)^4} \left[ \frac{16\pi^2 L}{\Lambda} \right]^{\epsilon/4}. \quad (5.2)$$

Such a scaling relation offers a guideline for the interpretation of experimental data and particularly, recent Monte Carlo data [22] for  $S^2$ . In view of the reduction of  $\Lambda$  due to the presence of  $u_0$  (see Appendix C), which is an unknown function, Eq. (5.1) is not the most convenient form that can be used. To avoid this problem, we may use the variable  $\bar{n}$  instead of  $\Lambda$ . In general, the relation

$$\bar{n} = \Lambda(u_0)L \quad (5.3)$$

is valid for large  $\Lambda L$ , despite the correction of  $\Lambda$  due to  $u_0$ . This can be shown by differentiating the partition function. Thus we propose to use

$$\bar{S}^2 \sim \frac{L}{\bar{n}^{1/2}} z^{2(4\nu-1)/\epsilon}, \quad (5.4)$$

with

$$z = \frac{u_0 \bar{n}^2}{(4\pi)^4 L^2} \left[ \frac{16\pi^2 L^2}{\lambda^2 \bar{n}} \right]^{\epsilon/4}, \quad (5.5)$$

which should be a more convenient scaling form for practical use. It is interesting to note that the combination of the parameters  $u_0 L^{\epsilon/4}$  also appears in the result of the Flory-type argument [11,20]. A similar situation exists in the theory of linear polymers, for which the Flory argument [1] yields the appropriate scaling parameter  $u_0 L^{(4-D)/2}$ .

We have also deduced the first-order term in the  $\epsilon$  expansion for the critical exponents  $\nu$  and  $\theta$ . These results agree with the results of Lubensky and Isaacson [7], although these authors used a completely different approach. While the difficulties in evaluating the Feynman diagram for the  $nm$ -component  $\phi$  field variable in Lubensky and Isaacson's theory [7] is avoided, our approach has its own difficulties in deriving the correlation functions  $G_l$ . The  $\epsilon$  expansion for  $\nu$  and  $\theta$  themselves, however, is probably less useful in the  $D=3$  case; the parameter  $\epsilon=8-3=5$  is probably too large to be considered as an expansion parameter.

It is the complication of branching structures that makes the calculation in this paper more difficult in comparison to that for linear polymers, although the procedures are quite similar. Extending our calculation to order  $\epsilon^2$  should be straightforward but tedious; one would need the expression for the end-to-end correlation function  $G_8$  with eight interior points. Such a study is important to further confirm our scaling assumption in Eqs. (5.1) and (5.2), which is based on a first-order expansion.

#### ACKNOWLEDGMENTS

This work was supported by the National Science and Engineering Research Council of Canada. S.M.C. was also supported partially by the University of Waterloo.

#### APPENDIX A: STRUCTURE FACTOR AND RADIUS OF GYRATION

In this appendix we calculate the mean-square radius of gyration  $S^2$  of noninteracting randomly branched polymers. Instead of deriving  $S^2$  from the Kramers theorem [25], as has been done before [5], we use the more basic approach of calculating the structure factor  $\mathcal{S}^{(0)}(\mathbf{k}; L)$ .

With the substitution of the explicit form of  $\tilde{G}_2$  in Eq. (3.25),  $\mathcal{S}^{(0)}(\mathbf{k}; p)$  takes the form

$$\tilde{\mathcal{S}}_B^{(0)}(\mathbf{k}, p) = \frac{\tilde{G}_0^2(0; p) \tilde{G}_0(\mathbf{k}; p)}{[1 - \Lambda^2 \tilde{G}_0^2(0; p)][1 - \Lambda^2 \tilde{G}_0(0; p) \tilde{G}_0(\mathbf{k}; p)]^2}. \quad (A1)$$

At  $\mathbf{k}=\mathbf{0}$ , we have

$$\tilde{\mathcal{S}}_B^{(0)}(0; p) = \frac{\tilde{G}_0^3(0; p)}{[1 - \Lambda^2 \tilde{G}_0^2(0; p)]^3}. \quad (A2)$$

Performing the inverse Laplace transformation yields

$$\mathcal{S}_B^{(0)}(0; L) = \frac{L}{2\Lambda} I_1(2\Lambda L), \quad (A3)$$

where  $I_m$  is the  $m$ th-order modified Bessel function of the first kind. Comparing with the expression of the partition function

$$G(L) = \frac{I_1(2\Lambda L)}{\Lambda L}, \quad (A4)$$

we have

$$\mathcal{S}_B^{(0)}(0; L) = \frac{L^2}{2} G(L). \quad (A5)$$

This result, of course, is consistent with the definition of  $\mathcal{S}_B(\mathbf{k}, L)$ , Eq. (3.24).

The numerator of the right-hand side of Eq. (3.23) can be obtained by using Eq. (A1)

$$-\frac{1}{D} \sum_{i=1}^D \frac{\partial^2 \tilde{\mathcal{S}}_B^{(0)}(\mathbf{k}, p)}{\partial k_i^2} \Big|_{\mathbf{k}=\mathbf{0}} = \frac{2\tilde{G}_0^4(0; p)[1 + \Lambda^2 \tilde{G}_0^2(0; p)]}{[1 - \Lambda^2 \tilde{G}_0^2(0; p)]^4}. \quad (A6)$$

Performing the inverse Laplace transformation of Eq. (A6) and substituting the result into the expression for  $S^2$  in Eq. (3.23), we have

$$\bar{S}^2 = \frac{LD}{2} \left[ \frac{\pi L}{\Lambda} \right]^{1/2} f(2\Lambda L), \quad (A7)$$

where

$$f(z) = \frac{I_{3/2}(z) - 2(2/\pi z)^{1/2} I_0(z) + (2/z) I_{1/2}(z)}{I_1(z)}, \quad (A8)$$

which has the following asymptotic behavior:

$$f(z) = \begin{cases} 2(z/2\pi)^{1/2}/3, & z \rightarrow 0 \\ 1, & z \rightarrow \infty \end{cases}. \quad (A9)$$

Note that  $\overline{S^2}$  is proportional to  $L^{1/2}$  at large  $\Lambda L$ , so that the mean-field critical exponent  $\nu_{\text{MF}} = \frac{1}{4}$ . This is the same result as that obtained by Zimm and Stockmayer [4] and de Gennes [5] before.

However, we are unable to use (A8) to recover exactly the expression for  $\overline{S^2}$  deduced based on the Kramers theorem [25], as prescribed by de Gennes [5]. From the Kramers theorem, one would obtain  $\overline{S^2}$  in the same function form as in Eq. (A7), however, with  $f(z)$  replaced by

$$f'(z) = \frac{I_{1/2}(z) - 2(2/\pi z)^{1/2} I_1(z)}{I_2(z)}. \quad (\text{A10})$$

The function  $f'(z)$  has the same asymptotic behavior given by Eq. (A9), but differs from  $f(z)$  in the intermediate region of  $z$ .

## APPENDIX B: CORRELATION FUNCTION

In this appendix the algebraic expressions for the  $(2+l)$ -point correlation function ( $l=2,3,4$ ) in the Fourier-Laplace space, which are used in Sec. III, are listed.

For  $l=2$ , we have generally

$$\begin{aligned} \tilde{G}_2(\mathbf{k}_1, \mathbf{k}_2; \mathbf{k}_3, \mathbf{k}_4; p) &= \tilde{G}_0(\mathbf{k}_1; p) \tilde{G}_0(\mathbf{k}_2; p) Y(\mathbf{k}_3; p) Y(\mathbf{k}_4; p) \\ &\times \{ \tilde{G}_0(\mathbf{k}_1 + \mathbf{k}_3; p) + \tilde{G}_0(\mathbf{k}_1 + \mathbf{k}_4; p) \\ &\quad + \Lambda^2 \tilde{G}_0(0; p) \tilde{G}_0(\mathbf{k}_3 + \mathbf{k}_4; p) [ \tilde{G}_0(\mathbf{k}_3; p) + \tilde{G}_0(\mathbf{k}_4; p) ] Y(\mathbf{k}_3 + \mathbf{k}_4; p) \} (2\pi)^D \delta(\mathbf{k}_1 + \mathbf{k}_2 + \mathbf{k}_3 + \mathbf{k}_4), \end{aligned} \quad (\text{B1})$$

where

$$Y(\mathbf{k}; p) = \frac{1}{1 - \Lambda^2 \tilde{G}_0(0; p) \tilde{G}_0(\mathbf{k}; p)}. \quad (\text{B2})$$

In particular, in the paper we used

$$\tilde{G}_2(0, 0; \mathbf{k}, -\mathbf{k}; p) = 2\tilde{G}_0^2(0; p) \tilde{G}_0(\mathbf{k}; p) Y(0; p) Y^2(\mathbf{k}; p). \quad (\text{B3})$$

For  $l=3$ , we have

$$\begin{aligned} \tilde{G}_3(0, 0; \mathbf{k}, -\mathbf{k}, 0; p) &= 2\tilde{G}_0^2(0; p) \tilde{G}_0(\mathbf{k}; p) Y^2(0; p) Y^2(\mathbf{k}; p) \\ &\times [ \tilde{G}_0(0; p) Y(0; p) Z(0; p) + \tilde{G}_0(0; p) Y(\mathbf{k}; p) Z(\mathbf{k}; p) + \tilde{G}_0(\mathbf{k}; p) Y(\mathbf{k}; p) Z(\mathbf{k}; p) ], \end{aligned} \quad (\text{B4})$$

where

$$Z(\mathbf{k}; p) = 1 + \Lambda^2 \tilde{G}_0(0; p) \tilde{G}_0(\mathbf{k}; p). \quad (\text{B5})$$

This formula is used to obtain Eq. (3.22), where the  $\mathbf{k}$  vectors of the two external ends and one interior point have been set to zero.

For  $l=4$ , we have

$$\begin{aligned} \tilde{G}_4(0, 0; \mathbf{k}, -\mathbf{k}, \mathbf{q}, -\mathbf{q}; p) &= 2\tilde{G}_0^2(0; p) Y(0; p) Y^2(\mathbf{k}; p) Y^2(\mathbf{q}; p) \\ &\times \{ 2\tilde{G}_0(0; p) \tilde{G}_0(\mathbf{k}; p) \tilde{G}_0(\mathbf{q}; p) Y(0; p) [ Y(\mathbf{k}; p) Z^2(\mathbf{k}; p) + Y(\mathbf{q}; p) Z^2(\mathbf{q}; p) + 2\Lambda^2 \tilde{G}_0^2(0; p) Y(0; p) ] \\ &\quad + Z(\mathbf{k}; p) Z(\mathbf{q}; p) [ \tilde{G}_0(\mathbf{k}; p) + \tilde{G}_0(\mathbf{q}; p) ] [ \tilde{G}_0(\mathbf{k}; p) Y(\mathbf{k}; p) + \tilde{G}_0(\mathbf{q}; p) Y(\mathbf{q}; p) ] \\ &\quad \times [ \tilde{G}_0(\mathbf{k} + \mathbf{q}; p) Y(\mathbf{k} + \mathbf{q}; p) + \tilde{G}_0(\mathbf{k} - \mathbf{q}; p) Y(\mathbf{k} - \mathbf{q}; p) ] \\ &\quad + \Lambda^2 \tilde{G}_0(0; p) [ \tilde{G}_0(\mathbf{k}; p) + \tilde{G}_0(\mathbf{q}; p) ]^2 [ \tilde{G}_0^2(\mathbf{k} + \mathbf{q}; p) Y^2(\mathbf{k} + \mathbf{q}; p) + \tilde{G}_0^2(\mathbf{k} - \mathbf{q}; p) Y^2(\mathbf{k} - \mathbf{q}; p) ] \}. \end{aligned} \quad (\text{B6})$$

This formula is used to obtain Eq. (3.27).

## APPENDIX C: CRITICAL DIMENSIONALITY

As we have indicated in the discussion of the perturbation theory, the model may be transformed to a field theory that is solved perturbatively by calculating the various correlation functions. To one-loop order, the end-to-end distribution function  $\tilde{G}$  is given by

$$\tilde{G}(\mathbf{k}; p) = \tilde{G}_0(\mathbf{k}; p) - u_0 \tilde{G}_0^2(\mathbf{k}; p) \int \frac{d^D \mathbf{q}}{(2\pi)^D} \frac{\tilde{G}_0(\mathbf{k} + \mathbf{q}; p) + \Lambda^2 \tilde{G}_0(0; p) [ \tilde{G}_0(\mathbf{q}; p) - \tilde{G}_0(\mathbf{k} + \mathbf{q}; p) ]}{[ 1 - \Lambda^2 \tilde{G}_0^2(0; p) ] [ 1 - \Lambda^2 \tilde{G}_0(0; p) \tilde{G}_0(\mathbf{q}; p) ]^2}. \quad (\text{C1})$$

Maintaining the dominating term that contributes most significantly for large  $L$ , we have

$$\begin{aligned} \tilde{G}(\mathbf{k}; p) = \tilde{G}_0(\mathbf{k}; p) - \frac{u_0 \tilde{G}_0^2(\mathbf{k}; p)}{(p^2 - 4\Lambda^2)^{1/2}} \\ \times \int \frac{d^D \mathbf{q}}{(2\pi)^D} \frac{1}{[\mathbf{q}^2 + (p^2 - 4\Lambda^2)^{1/2}]^2}. \end{aligned} \quad (C2)$$

By mapping the model to a spin field theory, we can define the two-point vertex function  $G^{-1}$  as

$$\begin{aligned} \tilde{G}^{-1}(\mathbf{k}; p) = \tilde{G}_0^{-1}(\mathbf{k}; p) \\ + \frac{u_0}{(p^2 - 4\Lambda^2)^{1/2}} \\ \times \int \frac{d^D \mathbf{q}}{(2\pi)^D} \frac{1}{[\mathbf{q}^2 + (p^2 - 4\Lambda^2)^{1/2}]^2}. \end{aligned} \quad (C3)$$

The inverse of the susceptibility is given by

$$\begin{aligned} \chi^{-1} = \tilde{G}_0^{-1}(0; p), \\ \chi^{-1} = \frac{p+t}{2} + \frac{u_0}{t} \int \frac{d^D \mathbf{q}}{(2\pi)^4} \frac{1}{(\mathbf{q}^2 + t)^2}, \end{aligned} \quad (C4)$$

where for convenience, we denote  $t = (p^2 - 4\Lambda^2)^{1/2}$ . The critical dimensionality is determined by examining Eq. (C4).

When transforming Eq. (C4) back to the  $L$  space by using the inverse Laplace transformation for  $p$ , we must consider an integral path in the complex  $p$  plane parallel to the imaginary axis and on the right-hand side of the line defined by  $p = 2\Lambda$ . In particular, the large- $L$  behavior of  $\chi^{-1}$  mainly comes from the part of the integral path close to the point  $(2\Lambda, 0)$ . The straight line defined by  $p = 2\Lambda$  produces the exponential factor  $\exp(2\Lambda L)$  as shown by explicit calculations [see Eq.

(3.12)]. Note that Daoud and Joanny [21] pointed out that a similar propagator, valid for large  $L$ , can be used in a similar context and that Parisi and Sourlas [8] considered a propagator that produces the same singularity structure.

The integral in Eq. (C4), however, is ill defined; an upper cutoff of order  $1/a$  must be imposed to prevent ultraviolet divergences appearing at  $D = 4, 6, 8, \dots$ . Furthermore, when the "critical point"  $t = 0$  is approached,  $\chi^{-1}$  does not approach the unperturbed linear dependence on  $t$ , shown in Eq. (C4) by the first term. Defining shifts for the parameters  $p$  and  $\Lambda$ ,

$$\bar{p} = p - 4u_0 \int \frac{d^D \mathbf{q}}{(2\pi)^D} \frac{1}{q^6}, \quad (C5)$$

$$\bar{\Lambda} = \Lambda - \frac{u_0}{2\Lambda} \int \frac{d^D \mathbf{q}}{(2\pi)^D} \frac{1}{q^4} - \frac{pu_0}{\Lambda} \int \frac{d^D \mathbf{q}}{(2\pi)^D} \frac{1}{q^6}, \quad (C6)$$

we may write

$$\begin{aligned} \chi^{-1} = \frac{\bar{p} + (\bar{p}^2 - 4\bar{\Lambda}^2)^{1/2}}{2} + 3u_0 t \int \frac{d^D \mathbf{q}}{(2\pi)^D} \frac{1}{(\mathbf{q}^2 + t)^2 q^4} \\ + 2u_0 t^2 \int \frac{d^D \mathbf{q}}{(2\pi)^4} \frac{1}{(\mathbf{q}^2 + t)^2 q^6}. \end{aligned} \quad (C7)$$

We note from Eq. (C7) that  $\chi^{-1}$  remains finite in the limit of the ultraviolet cutoff  $1/a$  becoming infinite, provided  $D < 8$ . This implies that the upper critical dimension of the model is  $D_c = 8$ . We also note that the parameters  $p$  and  $\Lambda$  are shifted down from their original values. This shift depends highly on the cutoff  $1/a$ , as well as the method of implementing the cutoff. The ultraviolet divergences in the original integral [Eq. (C4)] at  $D = 4$  and  $6$  are absorbed into the definitions of the parameters  $\bar{p}$  and  $\bar{\Lambda}$ . Finally, we note that the integral in Eq. (C7) still contains a singularity when  $D_c = 8$  is approached. This singularity must be removed by using the renormalization group scheme discussed in the text.

- 
- [1] P. G. de Gennes, *Scaling Concepts in Polymer Physics* (Cornell University Press, Ithaca, 1979).
- [2] P. J. Flory, *Principle of Polymer Chemistry* (Cornell University Press, Ithaca, 1971).
- [3] K. F. Freed, *Renormalization Group Theory of Macromolecules* (Wiley, New York, 1987), and references therein.
- [4] B. H. Zimm and W. H. Stockmayer, *J. Chem. Phys.* **17**, 1301 (1949).
- [5] P. G. de Gennes, *Biopolymer* **6**, 715 (1968).
- [6] M. Daoud and A. Lapp, *J. Phys. Condens. Matter* **2**, 4021 (1990).
- [7] T. C. Lubensky and J. Isaacson, *Phys. Rev. A* **20**, 2130 (1979).
- [8] G. Parisi and N. Sourlas, *Phys. Rev. Lett.* **46**, 871 (1981).
- [9] Y. Shapir, *Physica D* **15**, 129 (1985).
- [10] A. Bunde, S. Havlin, and M. Porto, *Phys. Rev. Lett.* **74**, 2714 (1994).
- [11] A. M. Gutin, A. Y. Grosberg, and E. I. Shakhnovich, *Macromolecules* **26**, 1293 (1993).
- [12] A. M. Gutin, A. Y. Grosberg, and E. I. Shakhnovich, *J. Phys. A* **26**, 1037 (1993).
- [13] A. Y. Grosberg, A. M. Gutin, and E. I. Shakhnovich, *Macromolecules* **28**, 3718 (1995).
- [14] D. Gaunt and S. Flesia, *J. Phys. A* **24**, 3655 (1991).
- [15] E. J. van Rensburg and N. Madras, *J. Phys. A* **25**, 303 (1992), and references therein.
- [16] P. G. de Gennes, *Riv. Nuovo Cimento* **7**, 366 (1977).
- [17] Y. Oono, T. Ohta, and K. F. Freed, *J. Chem. Phys.* **74**, 6458 (1975); T. Ohta, Y. Oono, and K. F. Freed, *Phys. Rev. A* **25**, 2801 (1982).
- [18] T. A. Witten and L. Schafer, *J. Phys. A* **11**, 1843 (1978); *J. Chem. Phys.* **74**, 2582 (1981).
- [19] J. Isaacson and T. C. Lubensky, *J. Phys. Lett.* **41**, L469 (1980).
- [20] M. Daoud, P. Pincus, W. H. Stockmayer, and T. Witten, *Macromolecules* **16**, 1833 (1983).
- [21] M. Daoud and J. F. Joanny, *J. Phys.* **42**, 1359 (1981).

- [22] S.-M. Cui and Z. Y. Chen (unpublished).  
[23] S.-M. Cui and Z. Y. Chen (unpublished).  
[24] G. 't Hooft and M. Veltman, Nucl. Phys. B **44**, 189 (1972);  
see also D. J. Amit, *Field Theory, The Renormalization Group and Critical Phenomena* (McGraw-Hill, New York, 1978).  
[25] H. A. Kramers, J. Chem. Phys. **14**, 415 (1946).  
[26] H. Yamakawa, *Modern Theory of Polymer Solutions* (Harper and Row, New York, 1971).